A Heuristic Framework for Sources Detection in Social Networks via Graph Convolutional Networks

Le Cheng, Peican Zhu, *Member, IEEE*, Chao Gao, Zhen Wang, *Fellow, IEEE*, and Xuelong Li, *Fellow, IEEE*

***Abstract*—The rapid development of social networks has given opportunities for rumors to disturb the order of society. However, due to the diversity and complexity of users and information dissemination dynamics, localizing the rumor sources in social networks is still a critical and crucial problem yet to be well solved. Recent years, although several methods have been proposed to attempt to solve this problem, they suffer from the contradiction between accuracy and model complexity. To detect information sources efficiently, this article propose a heuristic framework for sources detection (HFSD) in social networks via graph convolutional networks which handles three major challenges, including: 1) the diversity and complexity of users and information dissemination dynamics; 2) difficulty to detect multiple sources, especially without knowing the number of sources; and 3) the class imbalance problem caused by the large differences in sample size of sources and nonsources. Specifically, first, to counteract the diversity and complexity of users and information, different kinds of features of users and information are encoded in the raw feature vectors; second, to address multi-source detection, we adopt a binary classification in the last layer of model, which is different from the *n*-classification methods that are always applied to single-source scenario; finally, to solve the class imbalance problem, we design a balance mechanism which offsets the differences in sample size between the sets of sources and nonsources. Extensive experiments conducted on 12 real-world datasets demonstrate that HFSD can handle problems mentioned above and outperforms than state-of-the-art algorithms significantly.**

***Index Terms*—Class imbalance, graph convolutional networks (GCNs), information spreading, sources detection, user features.**

Manuscript received 6 April 2024; accepted 9 August 2024. This work was supported in part by the National Natural Science Foundation of China under Grant U22B2036, Grant 62025602, Grant 61976181, and Grant 62073263; in part by the Fok Ying-Tong Education Foundation, China, under Grant 171105; in part by the Technology Innovation Leading Program of Shaanxi under Grant 2023GXLH-086; in part by the Fundamental Research Funds for the Central Universities under Grant G2024WD0151; in part by the Open Research Subject of State Key Laboratory of Intelligent Game under Grant ZBKF-24-02; in part by the Innovation Foundation for Doctor Dissertation of Northwestern Polytechnical University under Grant CX2023068; and in part by the Tencent Foundation and XPLORER PRIZE. This article was recommended by Associate Editor L. Wang. *(Corresponding authors: Peican Zhu; Zhen Wang.)*

Le Cheng is with the School of Artificial Intelligence, Optics and Electronics and the School of Computer Science, Northwestern Polytechnical University, Xi'an 710072, Shaanxi, China.

Peican Zhu, Chao Gao, Zhen Wang, and Xuelong Li are with the School of iOPEN, Northwestern Polytechnical University, Xi'an 710072, Shaanxi, China (e-mail: ericcan@nwpu.edu.cn; nkzhenwang@163.com).

Color versions of one or more figures in this article are available at https://doi.org/10.1109/TSMC.2024.3448226.

Digital Object Identifier 10.1109/TSMC.2024.3448226

I. Introduction

THE MAJORITY of complex systems in the physical realm can be conceptualized as complex networks, exemplified by the surge in social networks over recent decades [1], [2], [3]. This evolution has significantly enhanced interpersonal communication, enabling individuals to effortlessly share their perspectives or access vital information at a reduced cost [4], [5], [6]. However, it has concurrently paved the way for the spread of malicious content; for example, the propagation of rumors can severely disrupt social harmony [7], [8], [9], [10]. Therefore, identifying these sources to curb their dissemination and mitigate their impact at the earliest opportunity bears substantial theoretical and practical importance [11], [12], [13].

In recent years, a number of seminal approaches have been introduced to identify information sources within complex networks. Traditionally, these existing methodologies for source localization can be categorized into three distinct classes: 1) complete observation-based methods; 2) sensor-based methods; and 3) snapshot-based methods [14]. For the complete observation-based methods, the status of each node within the network is known at any given time t during the propagation process; such approaches offer comprehensive knowledge for source detection (SD), yet the acquisition of detailed information poses significant challenges in practice. For the sensor-based methods, administrators initially deploy a number of observers within networks. Upon the outbreak and subsequent transmission of the propagation across these observers, dynamic information, including the times of infection and the directions of spread, is captured and furnished as input to various localization algorithms. Nonetheless, the predeployment of observers introduces a significant cost challenge that sensor-based methods must contend with. Furthermore, classic sensor-based approaches, such as maximum-likelihood estimator (MLE)-P [15], DISGE [16], and GSSI [17], detect sources based on the MLE. Given that MLE necessitates a comparison of the recorded data's similarity across different propagations, these methodologies are compelled to reconstruct the spreading process. This entails accurately modeling the propagation and identifying the spreading parameters—a task that often proves challenging in practical scenarios. Without knowing the propagation model and spreading parameters, snapshot-based methods, such as LPSI [18], EPA [19], and EC + CC [20], determine sources based on network snapshots. Such snapshots encapsulate the

state of every node at a specific moment, i.e., the instance when the propagation ceases. Subsequently, SD is conducted based on various established centrality metrics, for instance, source centrality theory [21], [22], eccentricity centrality [23], closeness centrality [24], etc. Although snapshot-based approaches are broadly applicable in scenarios involving the detection of multiple sources, experimental outcomes have shown that their accuracy leaves much to be desired [25].

In social networks, user diversity manifests through various dimensions, including activity levels and the breadth of social connections, which in turn affect their influence. Concurrently, the propagation of information within these networks is characterized by a high degree of randomness [26]. These multifaceted challenges significantly impede the process of accurately locating the sources of information or rumors, marking a complex hurdle in the field of source localization [27]. A pragmatic approach to address these challenges involves the fusion of multifactorial data through machine learning (ML) techniques. In recent advancements, ML-based methodologies have demonstrated substantial progress across numerous domains [28]. This progress is notably catalyzed by the advent of graph neural networks (GNNs), which adapt the principles of neural networks (NNs) for application within graph structures, inherently non-Euclidean spaces [29]. The development and implementation of graph convolutional networks (GCNs) have further expedited this evolution [30], with both GNNs and GCNs proving to be adept at learning effective node embedding representations through the integration of individual and adjacent node information. Source localization, while a burgeoning field of study, remains underexplored. Dong et al. [31] ventured into this domain by employing GCN for source localization and proposed the GCNs-based source identification (GCNSI) framework. This methodology hinges on the construction of node features through a generative algorithm, facilitating the detection of multiple sources with a model that remains computationally light. Despite these innovations, the challenge of class imbalance has led to less than optimal accuracy levels. Incorporating graph diffusion, strategies, such as invertible validity-aware graph diffusion (IVGD) [32] and source localization variational autoencoder (SL-VAE) [33], have been introduced, leveraging graph diffusion characteristics to enhance the fidelity of source localization. By adopting a graph diffusion learning mechanism, these approaches have attained superior accuracy. Nevertheless, this reliance on graph diffusion necessitates the incorporation of hard-to-obtain prior information, such as the initial number of sources or the paths of information diffusion, into the model training phase. Moreover, the intricate nature of these models contributes to increased computational demands, highlighting a critical area for future optimization and research.

In this article, we introduce a heuristic framework for sources detection (HFSD) in social networks, designed to navigate the diversity and complexity of users and information dissemination dynamics. This framework is engineered to address three pivotal challenges.

1) *Complexity in Modeling Information Diffusion:* The modeling of information diffusion processes is complicated by the diversity and complexity inherent to users and the dynamics of information spread. As illustrated in Fig. 1(a), the user base within a network exhibits significant heterogeneity in social attributes and influence levels. Additionally, the mechanisms underlying information propagation are marked by both complexity and randomness, as depicted in Fig. 1(b) and (c).
2) *Multisource Detection Difficulties:* Identifying multiple sources is particularly challenging, especially without knowing the number of sources. Detecting multiple sources has always been a difficult problem for sources localization, since the influence spheres of different sources may overlap.
3) *Class Imbalance:* The pronounced disparity in the sample sizes of sources versus nonsources presents a significant obstacle. Typically, the actual sources constitute a minor fraction of the network's population, which might lead to NN models overlooking this crucial subset and producing outcomes that directly contradicts the objective of SD.

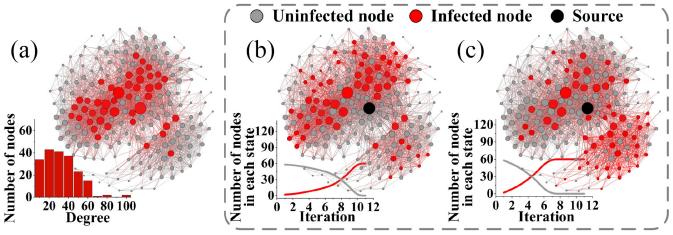

Fig. 1. Degree distribution and the differences in information dissemination process. Subgraph (a) represents the degree distribution while the nodes with significant influence were colored by red; subgraphs (b) and (c) show the information spreading process, as indicated, even starting from the same source, information spreads at different speeds and to different audiences.

To tackle these challenges, our framework adopts a novel approach. First, diverging from graph diffusion learning modules with high computational complexity, we encode various user and information features, including state, neighbor, structural, and diffusion features, into the raw feature vectors. This encoding process is designed to be flexible, allowing for the incorporation of additional features as required. Second, we employ a binary classification layer in our NN model, diverging from the traditional n-classification approaches typically used in single-source scenarios. This method entails processing each node through a binary classifier, rather than selecting one from n potential nodes, facilitating the identification of multiple sources without prior knowledge of their number. Finally, to mitigate the class imbalance issue, we introduce a balancing mechanism that adjusts the weights inversely proportional to the class sample sizes. This adjustment diminishes the influence of over represented classes while amplifying that of underrepresented ones, such as the actual sources. Through these innovations, HFSD presents a comprehensive solution for detecting information sources within social networks, effectively balancing accuracy with model complexity.

The main contributions of this article are summarized as follows.

1) Different perspectives of user and information features are encoded in the process of sources detection, diverging from graph diffusion learning modules characterized by high computational complexity. This divergence results in a more lightweight model, thereby saving computational costs.
2) To address multisource detection, we adopt a binary classification in the last layer of NN model, which is different from the n-classification methods that are always applied to single-source scenario.
3) For the class imbalance problem, we design a balance mechanism which offsets the differences in sample size between the sets of sources and nonsources; the balance mechanism can also be applied to other classification tasks facing the class imbalance problem.

In summary, the remainder of this manuscript is organized as follows. Section II lists the related works about source localization proposed in recent decades. Details of the proposed HFSD and necessary symbol notations are provided in Section III. In Section IV, extensive experiments are conducted and corresponding results are presented with sufficient analyses. Eventually, we conclude this article and also make a comprehensive discussion in Section V.

II. Related Works

In this section, we provide an overview of the literature pertaining to source localization, categorized into two primary areas: 1) different information diffusion models and 2) influential works in SD published recent years.

A. Information Diffusion Model

Within the domain of existing SD methodologies, several classical diffusion models are widely employed to simulate the spread of information. For instance, infection-based models encompass the susceptible–infected (SI) [34], SI-recovered (SIR) [35], and SI-susceptible (SIS) models [36], [37]. These models characterize nodes within the network with three distinct states: 1) susceptible (S), wherein the node remains ignorant and susceptible to activation by infected nodes; 2) infected (I), signifying activation, with the potential to transition into the R state in the SIR model or back to the S state in the SIS model; and 3) recovered (R), indicating nodes that have recovered and are no longer susceptible to activation. Furthermore, to model the process of information dissemination, the influence-based independent cascade (IC) [38] and linear threshold (LT) [39] models have been introduced. In the IC model, each informed node has precisely one opportunity to activate its uninformed neighbors, while in the LT model, uninformed nodes become activated if the cumulative influence from all their informed neighbors exceeds a predetermined threshold.

B. Source Detection Methods

Different kinds of SD methods have emerged in recent decades. Based on MLE, MLE-P addresses single-SD according to the infection time recorded by observers [15]. As an improvement of MLE-P, DISGE considers the direction information when propagation transits over observers [16]. To apply MLE to multisource scenario, SCCE divides the graph into several source candidate clusters and GSSI picks the source in each cluster [17]. However, since MLE needs to estimate the similarity between information vectors recorded by observers, these sensor-based methods have to reconstruct the propagation process, entailing precise determination of information diffusion models and spreading parameters, which is usually difficult in reality. From a different perspective, snapshot-based methods detect the source without knowing the underlying propagation model and parameters. LPSI achieves multisource detection via a label propagation mechanism: network snapshots taken after propagation cessation are annotated with label values corresponding to node states, iteratively refined until convergence, with source nodes identified based on local prominence [18]. Since source nodes are first infected, EPA calculates the age of every infected node iteratively and selects the oldest one as source [19]. Both LPSI and EPA detect source nodes through the source centrality theory [22], from a different and classic perspective, EC + CC localizes source node by eccentricity centrality and closeness centrality [20]. While snapshot-based methods demand less prior information compared to sensor-based counterparts, their localization accuracy often falls short of expectations.

Recent years, several ML-based methods have been developed for source localization. Dong et al. [31] proposed a deep-learning-based model, namely, GCNSI, in which node features are initially calculated and contacted through a generation algorithm before being fed into the GCN layers. This model is lightweight and capable of detecting multiple sources. From a different perspective, GCSSI [40] concentrates on the last infected users, i.e., the wavefront, and proposes a sequence-to-sequence model for source identification. However, both GCNSI and GCSSI grapple with the challenge of class imbalance, i.e., a significant disparity in sample sizes between source and nonsource sets, thus impacting their accuracy. In light of the information diffusion process, Wang et al. [32] introduced IVGD, an invertible graph diffusion model that learns both forward and inverse diffusion processes to facilitate SD. Since different sources may lead to the same information diffusion patterns, Ling et al. [33] presented SL-VAE, designed to localize sources in arbitrary diffusion patterns by considering information diffusion dynamics. While IVGD and SL-VAE boast commendable accuracy levels, they necessitate elusive prior information, such as the number of sources or information diffusion paths in the model training phase. Moreover, model complexity emerges as a pertinent concern in their implementation.

Hence, the development of a heuristic framework for SD in social networks becomes imperative, ideally striking a balance between accuracy and model complexity.

III. Proposed HFSD Framework

In this section, we initially outline the sources localization problem, followed by a comprehensive elucidation of our proposed HFSD. Concurrently, we present the requisite notations, succinctly summarized in Table I.

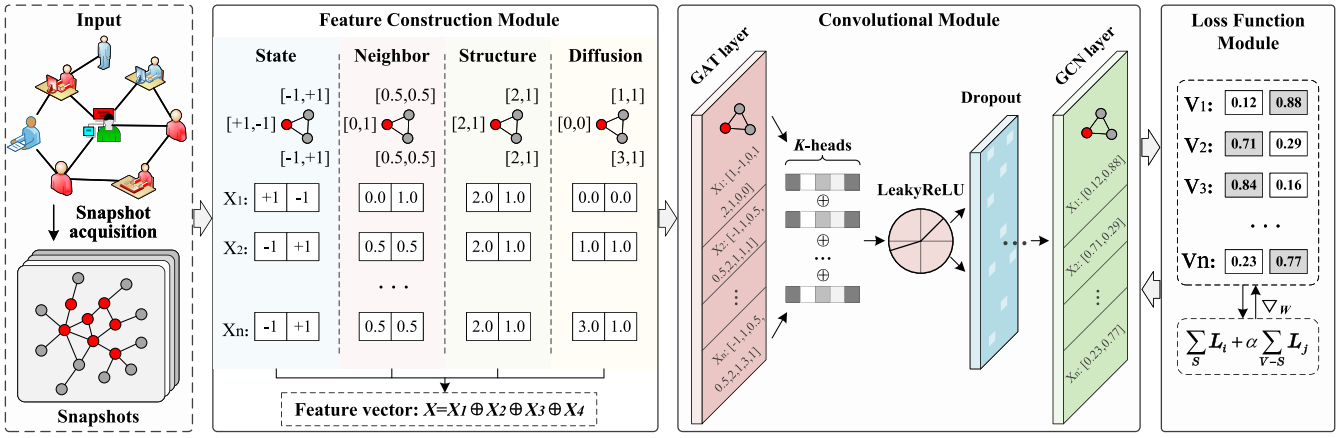

Fig. 2. Framework of the proposed HFSD. Feature construction module encodes the feature vector from different aspects according to the network snapshots and information diffusion process, convolutional module learns the node representations through several GAT and GCN layers, and loss function module calculates the classification loss by the designed balance mechanism and updates the parameter matrix through gradient.

TABLE I
PARAMETER NOTATION USED IN THIS ARTICLE

Notation	Interpretation
$G(V, E)$	The undirected graph
$G'(V, E)$	The infected graph
$\|V\|$	The number of nodes
$\|E\|$	The number of edges
$\langle k \rangle$	The average degree
p	Spreading rate
Y_i	The state of node v_i
T_i	The time at which node v_i was activated
S	The source set
$\widehat{S}$	The detected source set
A	Adjacency matrix of G
X	The feature matrix
W	The trainable parameter matrix
K	The number of attention heads

A. Problem Description

In practice, the social networks can be described as $G = (V, E)$, where V ($V = \{v_1, v_2, \ldots, v_n\}$) and E ($E = \{(v_i, v_j) \mid v_i, v_j \in V, i \neq j\}$) represent the sets of users (i.e., the nodes) and the connections among them (i.e., the edges), respectively. The numbers of nodes in V and edges in E are provided as $|V|$ and $|E|$, respectively. We define A ($A_{ij} \in \{0, 1\}^{n \times n}$) as the adjacency matrix of G, where

$$A_{ij} = \begin{cases} 1, & (v_i, v_j) \in E \\ 0, & \text{otherwise.} \end{cases} \tag{1}$$

The propagation phenomenon in social networks are usually started by several sources which are represented as $S = \{s_1, s_2, \ldots, s_m\}$, where m indicates the number of real sources. After the dissemination process being triggered by sources, the informed nodes try to affect their un-informated neighbors through existing edges. For example, once users believe in a rumor, they repost it to their friends. When the propagation has reached a certain stage deserving attention, a snapshot $G'(V, E, T)$ can be obtained, which includes the states of nodes and the time when the nodes are activated. Accordingly, the SD problem can be formulated as

$$SD : \hat{S} = f\big(G'(V, E, T)\big) \tag{2}$$

where T indicates the set of timestamps when the nodes are activated, $f(\cdot)$ represents the corresponding SD methods, and $\hat{S}$ is the detected source set.

B. Details of the Proposed HFSD

In this section, we address the challenge of detecting multiple sources in social networks by introducing an HFSD. This framework aims to overcome the diversity and complexity of users and information dissemination dynamics effectively. Fig. 2 shows the comprehensive schematic of the proposed model. As depicted, the framework encompasses three primary modules: 1) the feature construction module; 2) the convolutional module; and 3) the loss function module.

Within the feature construction module, we integrate a variety of information types into the feature vector, as shown in Fig. 2. To maintain clarity, our focus primarily lies on incorporating the node's state information, neighbors' information, network structural information, and diffusion information. For example, considering a specific node v_i, the constituents of the raw feature vector X_i could include the following.

1) Node's State Information (X_i^1): In a given network $G(V, E)$, a snapshot captured at the cessation of the propagation process is denoted as $G'(V, E)$. Within this snapshot G', any node v_i can be in one of two states: informed/activated or uninformed/inactivated. Accordingly, the state of node v_i, denoted by Y_i, is assigned a value of $+1$ for informed/activated states and 0 for uninformed/inactivated states. This categorization allows for the assignment of corresponding elements in X_i^1 based on the node's state

$$X_i^1 = \begin{cases} +1, & Y_i = 1 \\ -1, & \text{otherwise.} \end{cases} \tag{3}$$

2) Neighbors' Information (X_i^2): Building on the principles of source centrality theory, which posits that a node surrounded by a higher number of activated neighbors is more likely to be

the source of propagation [21], [22]. Hence, we innovatively define X_i^2 to be the proportion of activated neighbors among all neighbors of node v_i, thereby quantitatively assessing the likelihood of a node being the source based on its local network context

$$X_i^2 = \frac{\sum_{v_j \in N(v_i)} Y_j}{|N(v_i)|}. \tag{4}$$

3) Network's Structural Information (X_i^3): For exploring the structural information, several classical local centrality theories are proposed which is mainly based on considering n-order neighbors [23], [24]. For the convenience of reducing computational complexity, we only consider the scenario of $n = 1$ and the degree centrality here for explanation, i.e., $D_{v_i} = |N(v_i)|$. Moreover, aiming to minimize the numerical differences in the vector, we normalize X_i^3 as

$$X_i^3 = \frac{D_{v_i}}{\max_{v_j \in V} D_{v_j}}. \tag{5}$$

4) Diffusion Information (X_i^4): In practical scenarios, when users on social networks are influenced by a rumor and become persuaded, they are highly predisposed to share or repost this information to their neighbors via their network connections. Consequently, information pertaining to the diffusion process, including temporal data, such as timestamps, becomes indispensable for the identification of information sources. In this context, we incorporate the timestamp of user engagement with the rumor as a critical feature within our model, denoted as X_i^4, where $X_i^4 = T_i$.

It is worth mentioning that the elements in the above discussed feature vector can be enriched if necessary. For instance, for an activated node v_i, X_i^1 can be expanded to $X_i^1 = (+1, -1)$ for the purpose of enhancing the distinction, where -1 represents the anti-state of activation; $X_i^2 = (x, 1 - x)$, where $1 - x$ indicates the proportion of inactivated neighbors among all the neighbors; $X_i^3 = (\text{Deg}, Ecc, \ldots,)$ which denote the centrality measures being selected, such as degree centrality [41], eccentricity centrality [23], closeness centrality [24], etc.; $X_i^4 = (T, D)$, where D refers the direction during the information diffusion process. Then, these feature vectors are concatenated as $X_i = \|_{x=1}^4 X_i^x$.

For the convolutional module, we adopt the GCN which is effective in learning the node representation through integrating the information from the node itself and its neighbors. This technique has drawn an increasing interest on generalizing convolutions on the graph. Here, we consider a multilayer GCN model as the convolutional module by the layer wise propagation rule which can be formulated as

$$X^{(l+1)} = \sigma\left(\hat{A} X^{(l)} W^{(l)}\right) \tag{6}$$

where $\hat{A} = \widetilde{D}^{-(1/2)} \tilde{A} \widetilde{D}^{-(1/2)}$ indicates the normalized adjacency matrix (here, $\tilde{A} = A + I_n$ represents the nodes in graph are added with self connections and I_n is the identity matrix with n-dimension). $\widetilde{D}$ denotes the degree matrix of G and $\widetilde{D}_{ii} = \sum_j \tilde{A}_{ij}$. For the lth layer, $X^{(l)} \in \mathbb{R}^{n \times l_w}$ is the learnable node representation and $X^{(0)} = X$, l_w is the number of elements in node feature vector, $W^{(l)}$ is the trainable parameters matrix. $\sigma(\cdot)$ denotes the activation function, such as the ReLU function $\text{ReLU}(\cdot) = \max(0, \cdot)$. For instance, for a two layer GCN model, the propagation function can be represented as

$$f(X, A) = \text{softmax}\Big(\hat{A}\sigma(\hat{A}XW^{(0)})W^{(1)}\Big) \tag{7}$$

where the softmax$(\cdot)$ is a normalized exponential function and for a vector $\vec{z}$, we have

$$S(\vec{z})_i = \frac{e^{z_i}}{\sum_j e^{z_j}}. \tag{8}$$

Actually, the message propagation function defined above can be motivated by the first-order approximation of localized spectral filters on graphs [30], [42], [43]. To further improve the capability of learning node representations, we introduce the graph attention mechanism (GAT) to the convolutional layers. This addition allows nodes of varying degrees to assign specific weights to their neighbors, enabling a more dynamic and context-sensitive representation learning process [44]. Specifically, for node v_i and its neighbor v_j, the attention coefficient is calculated as

$$e_{ij} = \vec{a}\big(WX_i, WX_j\big). \tag{9}$$

In (9), $\vec{a} \in \mathbb{R}^{2l'_w}$ represents a weight vector. Consequently, the relative weight assigned to a neighbor of node v_i, in comparison to all neighbors of v_i, is determined as

$$\alpha_{ij} = \frac{\exp\big(\text{LeakyReLU}\big(\vec{a}^T\big[WX_i \| WX_j\big]\big)\big)}{\sum_{v_k \in N(v_i)} \exp\big(\text{LeakyReLU}\big(\vec{a}^T[WX_i \| WX_k]\big)\big)} \tag{10}$$

where LeakyReLU denotes an improved activation function based on ReLU which extends the activation (linear transformation) to negative numbers, $(\cdot)^T$ indicates the transposition and $||$ refers to the concatenation of two vectors. Hence, for each node, corresponding final output feature is calculated as

$$X_i' = \sigma\left(\sum_{v_j \in N(v_i)} \alpha_{ij} WX_j\right). \tag{11}$$

The GCN framework is further augmented by incorporating a multihead attention mechanism, wherein we deploy K parallel attention channels to process the graph's features. This approach allows for K independent executions of the attention mechanism as delineated in the previously discussed equation. Subsequently, the resultant feature vectors from each of these mechanisms are concatenated to form an enriched feature representation for each node. Formally, this can be represented as

$$X_i' = \|_{k=1}^K \sigma\left(\sum_{v_j \in N(v_i)} \alpha_{ij}^k W^k X_j\right). \tag{12}$$

Noticed that in (12), there are totally Kl_w elements in X_i'. Hence, on the last layer of our proposed model, X_i' is averaged accordingly

$$X_i' = \sigma\left(\frac{1}{K}\sum_{k=1}^K \sum_{v_j \in N(v_i)} \alpha_{ij}^k W^k X_j\right). \tag{13}$$

In the proposed model, we integrate the DropEdge technique to mitigate the risk of overfitting [45]. The DropEdge mechanism operates by randomly omitting a subset of edges from the graph in each training epoch. This stochastic alteration of the graph structure serves to diversify the propagation paths of information across the network, effectively regularizing the model by preventing the co-adaptation of node features. Formally, this process can be described as follows:

$$A' = A - A_{\text{drop}} \tag{14}$$

where A' represents the adjusted adjacency matrix after the removal of edges specified by A_{drop}. Concluding our model's architecture, the final layer is dedicated to a binary classification task, the representation vector for each node incorporates two probabilities, determining the likelihood of nodes being the source of information diffusion. This bifurcated probability approach allows for a nuanced assessment of each node's potential role in the spread of information.

Within the context of the loss function module, the initial step involves the application of the softmax function to the output vector generated by the convolutional module. This procedure ensures that the vector elements are normalized, with their sum equating to 1. In real-world propagation scenarios, the quantity of source nodes is typically finite, while the networks under consideration for propagation often encompass a vast scale, potentially exceeding thousands of nodes. This disparity gives rise to the issue of class imbalance, signifying pronounced differences in sample size between the set of source nodes and that of nonsource nodes. Consequently, the influence of source nodes on the loss metric may be diminished during the model training phase. To counteract the disparities in sample size, we propose a new balancing mechanism, detailed as follows:

$$\text{Loss} = \sum_{v_i \in S} L_i + \frac{|S|}{|V| - |S|} \sum_{v_j \in (V-S)} L_j + \lambda \|w\|_2 \tag{15}$$

where L denotes the standard cross-entropy loss; for a training sample x and its associated label y, the corresponding loss value is calculated as $L(x, y) = -\log(x) \times y$. Additionally, The term $\lambda\|w\|_2$ indicates the $L2$ regularization with a weight parameter λ. The coefficient $(|S|/[|V - S|])$ ensures uniform weighting across all nodes. Notably, the proposed balance mechanism can be extended to address class imbalance challenges encountered in other classification tasks.

In summary, the architecture of our proposed HFSD is depicted in Fig. 2. To manage computational resources efficiently, we employ batch training, wherein a batch of training samples is selected randomly for feature vector construction during each epoch. The feature construction module generates feature vectors, followed by the convolutional module learning node representations. Subsequently, the loss function module computes the loss and updates the parameters in W based on the gradient. The collaborative operation of these modules ensures that HFSD exhibits excellent adaptability and temporal–spatial efficiency. The summarized algorithm for HFSD is presented in Algorithm 1.

Algorithm 1: Illustration of the HFSD Algorithm

Input: The infected network $G' = (V, E)$; The timestamp vector T; The adjustable parameters.
Output: The detected source set $\widehat{S}$.

Construct the training set and test set containing N_{train} and N_{test} samples, respectively, through an arbitrary information diffusion model, the spreading rate $p \sim U(0, 0.3)$;
Training process:
for *epoch in epochs* **do**
  randomly select *batch* samples from training set;
  for *i in batch* **do**
    $X = \|_{x=1}^{4} X^x$
    $train\ accuracy = model(X, label)$
    $logits = softmax(model(X))$
    $loss \mathrel{+}= loss(logits, label)$
  $train\ accuracy \mathrel{/}= batch$
  $W \leftarrow \nabla_W(loss/batch)$
  if *early stopping met* **then**
    break;
Test process:
for *i in* N_{test} **do**
  $X = \|_{x=1}^{4} X^x$
  $accuracy \mathrel{+}= model(X, label)$
$accuracy \mathrel{/}= N_{test}$
return *accuracy*;

IV. Experimental Protocols

In this section, comprehensive experiments are conducted on 12 real-world datasets to assess the efficacy of the proposed HFSD. Corresponding results are compared against those obtained by state-of-the-art methods. Additionally, we explore the impact of various information diffusion models and data incompleteness on the performance of HFSD to demonstrate its robustness.

A. Preliminary

1) Datasets: Twelve real-world datasets of different scale are selected, encompassing six networks: Football [46], Jazz [47], Facebook [48], LastFM [49], Github [50], and DBLP [51]; alongside six social network information propagation datasets: Christianity [52], Memetracker [53], Android [52], Twitter [54], Douban [55], and Weibo [56]. The specific statistical details of these datasets are organized in Table II. For networks 1–6, $|V|$ and $|E|$ denote the number of nodes and edges within the networks, respectively, $\langle k \rangle$ represents the average degree, and CC signifies the clustering coefficient [57]. For datasets 7–12, #Users and #Links indicate the number of users on the social platforms and the count of friendships between them, #Cascades represents the quantity of distinct information obtained, and Avg. Length denotes the average length of these information propagation cascades.

2) Metrics: We define S and $\widehat{S}$ as the sets of true sources and detected ones, respectively. To comprehensively

TABLE II
CHARACTERISTICS OF THE SELECTED DATASETS

Id	Networks	$\|V\|$	$\|E\|$	$\langle k \rangle$	CC	Id	Datasets	#Users	#Links	#Cascades	Avg. Length
1	Football	115	613	10.66	0.40	7	Christianity	2897	35624	589	22.90
2	Jazz	198	2742	27.70	0.62	8	Memetracker	4709	209194	12661	16.24
3	Facebook	4039	88234	43.69	0.61	9	Android	9958	48573	679	33.30
4	LastFM	7624	27806	7.29	0.22	10	Twitter	12627	309631	3442	32.60
5	Github	37700	289003	15.33	0.17	11	Douban	23123	348280	10602	27.14
6	DBLP	317080	1049866	6.62	0.63	12	Weibo	46684	502400	18954	38.76

TABLE III
PERFORMANCE OF THE PROPOSED HFSD AND BASELINE METHODS ON DIFFERENT DATASETS

	Football			Jazz			Facebook			LastFM			Github			DBLP		
Methods	ACC	F1	AUC	ACC	F1	AUC	ACC	F1	AUC	ACC	F1	AUC	ACC	F1	AUC	ACC	F1	AUC
EPA	0.85	0.36	0.86	0.83	0.33	0.84	0.86	0.29	0.86	0.84	0.26	0.84	0.86	0.24	0.83	0.89	0.19	0.85
LPSI	0.83	0.37	0.87	0.85	0.35	0.87	0.87	0.25	0.83	0.86	0.23	0.83	0.85	0.21	0.81	0.84	0.15	0.86
GCNSI	0.85	0.25	0.81	0.84	0.26	0.83	0.86	0.10	0.72	0.81	0.09	0.68	0.81	0.07	0.65	0.82	0.05	0.60
IVGD	0.89	0.78	0.88	0.87	0.75	0.85	0.84	0.72	0.86	0.89	0.75	0.84	0.86	0.71	0.82	0.85	0.69	0.82
SL-VAE	0.91	0.81	0.89	0.85	0.82	0.88	0.86	0.76	0.85	0.90	0.74	0.83	0.89	0.75	0.86	0.91	0.71	0.86
HFSD	**0.95**	**0.89**	**0.95**	**0.93**	**0.91**	**0.94**	**0.89**	**0.85**	**0.91**	**0.95**	**0.90**	**0.96**	**0.93**	**0.82**	**0.91**	**0.94**	**0.81**	**0.92**
	Christianity			Memetracker			Android			Twitter			Douban			Weibo		
Methods	ACC	F1	AUC	ACC	F1	AUC	ACC	F1	AUC	ACC	F1	AUC	ACC	F1	AUC	ACC	F1	AUC
EPA	0.82	0.25	0.81	0.83	0.21	0.86	0.84	0.26	0.87	0.87	0.22	0.88	0.87	0.26	0.89	0.85	0.20	0.87
LPSI	0.83	0.26	0.82	0.85	0.25	0.87	0.86	0.25	0.86	0.85	0.23	0.89	0.86	0.24	0.87	0.87	0.25	0.84
GCNSI	0.84	0.11	0.72	0.81	0.12	0.71	0.82	0.10	0.73	0.84	0.09	0.69	0.83	0.14	0.71	0.86	0.13	0.72
IVGD	0.91	0.52	0.90	0.84	0.47	0.87	0.90	0.52	0.89	0.92	0.43	0.91	0.92	0.58	0.92	0.88	0.52	0.90
SL-VAE	0.92	0.53	0.92	0.85	0.46	0.88	0.89	0.56	0.90	0.91	0.48	0.92	0.91	0.56	0.90	0.89	0.54	0.89
HFSD	**0.94**	**0.63**	**0.95**	**0.88**	**0.58**	**0.91**	**0.93**	**0.61**	**0.92**	**0.95**	**0.59**	**0.96**	**0.95**	**0.71**	**0.94**	**0.91**	**0.67**	**0.92**

measure the performance of different methods, some widely used metrics are adopted, including Accuracy, F-Score, and AUC [18], [32], [58]. Accuracy indicates the proportion of samples that are correctly detected. F-Score is calculated as

$$F\text{-Score} = \left(1+\beta^2\right) * \frac{\text{Precision} * \text{Recall}}{\beta^2 * \text{Precision} + \text{Recall}} \tag{16}$$

where Precision represents the proportion of true sources in $\hat{S}$, and Recall represents the proportion of sources correctly detected in S. The parameter β is used to adjust the weights of Precision and Recall and is set to 1. AUC is determined by PFR and TPR, where PFR represents the proportion of nodes in $\hat{S}$ that are not sources, and TPR represents the proportion of true sources in $\hat{S}$. These evaluation metrics provide a comprehensive assessment of the performance of the methods employed in this study.

3) Baselines: For comparison, we select several approaches as baseline methods, including: EPA [19], LPSI [18], GCNSI [31], IVGD [32], and SL-VAE [33]. Here, EPA and LPSI are mainly used to detect multiple sources according to source centrality theory. GCNSI, IVGD, and SL-VAE are ML-based methods; specifically, GCNSI utilizes LPSI as the generation algorithm; IVGD and SL-VAE consider the information diffusion processes.

B. Comparison With State-of-the-Art Methods

To evaluate the effectiveness of our proposed method, we compare its performance with state-of-the-art methods on various real-world datasets. For networks 1–6, we employ the IC model to simulate the information diffusion process, with the spreading rate following a uniform distribution $p \sim U(0, 0.3)$. The number of sources is initialized based on the scale of the network. Specifically, for Football and Jazz, five sources are initialized, while for Facebook, LastFM, Github, and DBLP, the corresponding number is set to 10. The propagation process terminates when 30% of the nodes in the networks are informed or when the spreading process converges. For datasets 7–12, the first node in each propagation cascade is considered as the source node; nodes appearing in the cascades are deemed influenced by the information, while those not appearing are considered uninfluenced. In our proposed HFSD, we employ three graph attention (GAT) layers. The learning rate, weight decay, dropout rate, and number of hidden units are set to 1×10^{-3}, 5×10^{-4}, 0.1, and 500, respectively. The training and test datasets are divided in a proportion of 4:1. To manage computational resources, the batch size is set to 30, and the number of attention heads in the GAT model is set to 4 for the small-scale networks (Football, Jazz, Christianity, and Android), while for the other networks, these numbers are adjusted to 15 and 2, respectively. It is noteworthy that for HFSD, the number of sources, propagation model, and parameters are all unknown. Despite this, we provide the necessary parameters for some baseline methods, and the performance of these methods is reported based on their optimal results. The corresponding results are shown in Table III. Here, we consider several evaluation metrics, including Accuracy (ACC), F1-Score (F1), and AUC with the best performance being highlighted.

As shown in Table III, EPA and LPSI exhibit similar performance as they both rely on the source centrality theory. Their high ACC and AUC values suggest that the majority of real sources are correctly identified. However, their low

F1 scores stem from treating all suspicious nodes as propagation sources, resulting in numerous detected source sets. Among the ML-based methods, GCNSI performs the poorest due to severe effects of the class imbalance problem. The model tends to label most nodes in the network as source nodes, leading to the lowest F1 score among all methods. Given the high randomness of information propagation paths in reality, it becomes imperative to incorporate graph dissemination dynamics into the model. IVGD and SL-VAE, by considering the graph diffusion process, achieve superior accuracy. Our proposed HFSD exhibits the highest accuracy among all methods. Overall, the performance of all methods on small-scale networks generally surpasses that on larger networks. This is primarily because, under the same propagation scale, large-scale networks harbor a greater number of affected nodes compared to small-scale networks, necessitating the exclusion of more candidate nodes. As uncertainty increases, the accuracy of SD diminishes. Furthermore, across datasets 7–12, all methods exhibit lower F1 scores compared to networks 1–6. This disparity arises from datasets with only one source, resulting in an F1 score of 0 when not correctly identified. In summary, due to the consideration of various feature aspects and the efficiency of the designed class balance mechanism, our proposed HFSD demonstrates a 15%–25% improvement over methods based on the source centrality theory from a data standpoint. Moreover, its accuracy surpasses that of ML-based methods without considering the graph diffusion process by a factor of 4, and it achieves a 5%–15% enhancement over ML-based methods that do consider the graph diffusion process.

TABLE IV
EFFECTS OF DIFFERENT PROPAGATION MODELS

	Football			Jazz			Facebook		
Models	ACC	F1	AUC	ACC	F1	AUC	ACC	F1	AUC
SI	0.95	0.85	0.93	0.94	0.90	0.92	0.87	0.86	0.90
SIS	0.91	0.81	0.91	0.92	0.81	0.89	0.88	0.78	0.86
SIR	0.92	0.78	0.92	0.91	0.79	0.91	0.89	0.75	0.89
IC	0.95	0.89	0.95	0.93	0.91	0.94	0.89	0.85	0.91
LT	0.91	0.87	0.90	0.89	0.88	0.91	0.85	0.84	0.88
	LastFM			Github			DBLP		
Models	ACC	F1	AUC	ACC	F1	AUC	ACC	F1	AUC
SI	0.93	0.88	0.94	0.92	0.80	0.90	0.95	0.79	0.91
SIS	0.92	0.79	0.92	0.93	0.72	0.85	0.92	0.70	0.87
SIR	0.93	0.75	0.93	0.90	0.71	0.89	0.91	0.68	0.90
IC	0.95	0.90	0.96	0.93	0.82	0.91	0.94	0.81	0.92
LT	0.92	0.88	0.93	0.89	0.81	0.90	0.91	0.82	0.89

C. Effects of Different Information Diffusion Models

To evaluate the impact of employing different information diffusion models on the performance of our proposed HFSD, we employ various models to simulate the propagation process. Here, we incorporate two types of models: infection-based and influence-based models. For the infection-based models, we consider the SI model, SIS model, and SIR model. Meanwhile, for the influence-based models, we mainly focus on the IC model and LT model. In the SI, SIS, SIR, and IC models, the spreading rate of each node is randomly selected from 0 to 0.3, denoted as $p \sim U(0, 0.3)$. Additionally, the recovery rate of infected nodes in the SIS and SIR models is set to 0.03. Moreover, the threshold value of each node in the LT model is set to $\theta \sim U(0, 0.3)$. We terminate the propagation process when 30% of the nodes are informed or the spreading process reaches convergence. The results are summarized in Table IV.

As illustrated, a comprehensive evaluation reveals that the performance of the proposed HFSD exhibits a nuanced dependency on network scale and the underlying propagation model. Initially, it is observed that HFSD achieves marginally higher F1-Scores on networks of smaller scale compared to those of larger scale, primarily due to variations in the scale of activated nodes. Subsequently, our analysis indicates that the choice of propagation model exerts a relatively modest influence on HFSD's effectiveness. Specifically, HFSD's performance is slightly diminished under the SIS and SIR models. This decrement is attributed to the dynamics of these models, wherein informed nodes possess the capacity to recover, altering their original features, such as timestamps and node states. In the SIS model, recovered nodes may be reinfected, further complicating the source node detection process. Conversely, in the SIR model, once recovered, nodes are rendered immune to future infections, thereby altering the network's state and potentially obfuscating the source of propagation. Despite these challenges, the impact on HFSD's F1-Score remains limited. The empirical evidence amassed through our experiments corroborates the robust applicability of HFSD in practical scenarios, underscoring its resilience to variations in network scale and the dynamics of different propagation models.

D. Effects of Propagation Scale

In operational contexts, the variance in propagation scales poses significant challenges to the SD paradigm. This study delves into the impact of propagation scale on detection efficacy, through a comparative analysis involving the proposed HFSD model alongside established baseline methodologies, across diverse networks, such as Jazz, Facebook, GitHub, and DBLP. The propagation dynamics are simulated using the IC model, with the spreading rate governed by a uniform distribution, $p \sim U(0, 0.3)$. The simulation concludes, capturing a network snapshot, either when a predetermined proportion of nodes, namely, 10%, 30%, 50%, 70%, and 90% become informed, or upon the convergence of the propagation process. Subsequent to this, we employ the localization technique to ascertain the sources set. The effectiveness of the detection methods is quantified through the F1-Score metric, with the findings presented in Fig. 3.

As depicted in Fig. 3, there is a noticeable decline in the F1-Score across all datasets with the escalation of propagation scale. This trend can be attributed to the increased number of informed nodes over time, enlarging the sample size required for detection, consequently, elevating the complexity of the localization task. Notably, the performance of all methods on the Jazz and Facebook networks surpasses that observed on the GitHub and DBLP networks, a variance influenced by the differential count of informed nodes. Such

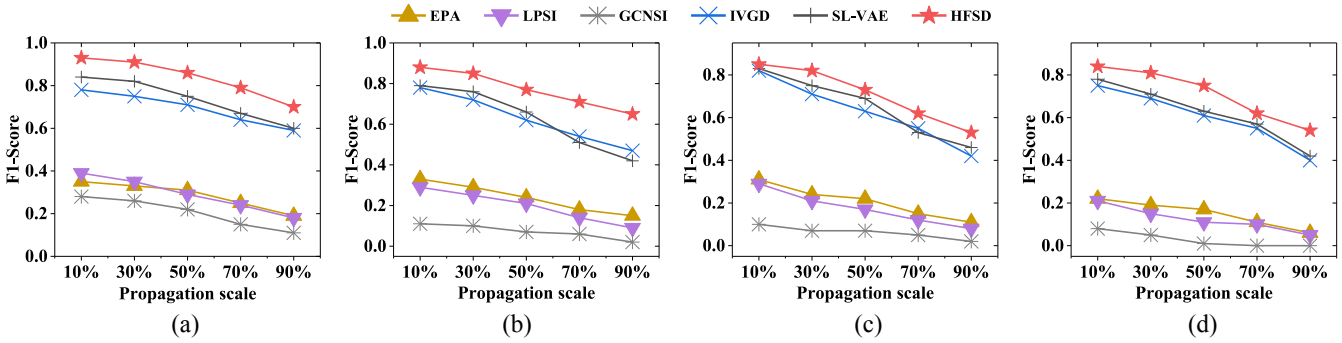

Fig. 3. Impact of propagation scale on the efficacy of SD algorithms across various networks. Here, we consider several datasets, including (a) Jazz, (b) Facebook, (c) Github, and (d) DBLP. The corresponding performance is measured through F1-Score.

findings underscore the criticality of early-stage SD within the propagation process. Among the baseline methods, GCNSI exhibits the lowest performance, significantly hampered by class imbalance issues. Methods predicated on the source centrality theory, such as EPA and LPSI, fare moderately, while those incorporating the propagation process, namely, IVGD and SL-VAE, achieve superior results. Across all datasets and propagation scales, HFSD consistently outperforms its counterparts, affirming its efficacy and robustness. This comparative analysis highlights HFSD's superiority in SD, regardless of the propagation scale, showcasing its practical utility and resilience in varied network environments.

E. Effects of Data Incompleteness

The majority of current methodologies for source localization operate under the assumption of data completeness. Nevertheless, in practical scenarios, the data acquired is often incomplete due to various factors, such as cost implications and the need to protect user privacy. For instance, observational data may lack comprehensive timestamps or detailed spreading paths, presenting significant challenges for accurate SD. To address these challenges, this study investigates the impact of data incompleteness on detection accuracy. Specifically, for networks 2–5, we evaluate the performance of the proposed HFSD and various baseline methods on selected networks under the IC model, incorporating varying degrees of data incompleteness. In the Jazz network, the propagation is initiated by five sources, while in the Facebook, LastFM, and Github networks, the number of sources is set at 10. The spreading rate within the IC model follows a uniform distribution $p \sim U(0, 0.3)$, and the propagation process is halted when 30% of the network's nodes are informed or upon the convergence of the spreading process. For datasets 3–6, each propagation cascade represents an independent information dissemination event, where the first node is the source and the subsequent nodes are those affected by the propagation. Nodes not appearing within a cascade are considered unaffected. To simulate data incompleteness, we randomly remove 10%, 15%, 20%, 25%, and 30% of the data from snapshots and use this incomplete observation as input to evaluate the algorithm's performance. The performance of baseline methods is determined based on their optimal configurations. The outcomes of these evaluations are depicted in Fig. 4.

As shown, a discernible trend emerges across all evaluated methods, where the F1-Scores decline in tandem with an increase in the rate of data incompleteness. This pattern primarily arises from the disruption caused by missing data during the model training process, which complicates the convergence to effective solutions. Furthermore, the influence of network scale is evident, with methods generally exhibiting superior performance on smaller networks as opposed to larger ones. This disparity is attributed to the greater number of nodes that must be accounted for in larger networks, which introduces increased uncertainty into the detection process. Notably, the proposed HFSD method consistently surpasses the performance of baseline methods under all conditions of data incompleteness. In comparison to other methods that account for the graph diffusion process, HFSD demonstrates an improvement in the F1-Score ranging from 3% to 15% across various incomplete ratios. This enhancement underscores the robustness of HFSD, affirming its resilience against the challenges posed by incomplete data.

F. Effects of the Number of GAT Layers and Hidden Units

The structural complexity of NNs, defined by the number of layers and hidden units, significantly influences their performance. This study, therefore, aims to elucidate the impact of these critical parameters, specifically the number of GAT layers and hidden units, on the effectiveness of our proposed HFSD model through comprehensive experiments on selected datasets. For networks 2–6, the IC model is employed to simulate the information diffusion process, with a spreading rate governed by $p \sim U(0, 0.3)$. In the Jazz network, five nodes are randomly chosen as sources; for the Facebook, LastFM, GitHub, and DBLP networks, the number of initialized sources is set at 10. The propagation is halted once 30% of the nodes are informed or the diffusion process reaches convergence. For datasets 8–12, each propagation cascade is treated as an independent diffusion event. Within the proposed HFSD framework, the number of GAT layers for smaller networks (such as Jazz, Facebook, LastFM, Memetracker, and Android) is adjusted between 2 and 8, while for larger networks (such as GitHub, DBLP, Twitter, Douban,

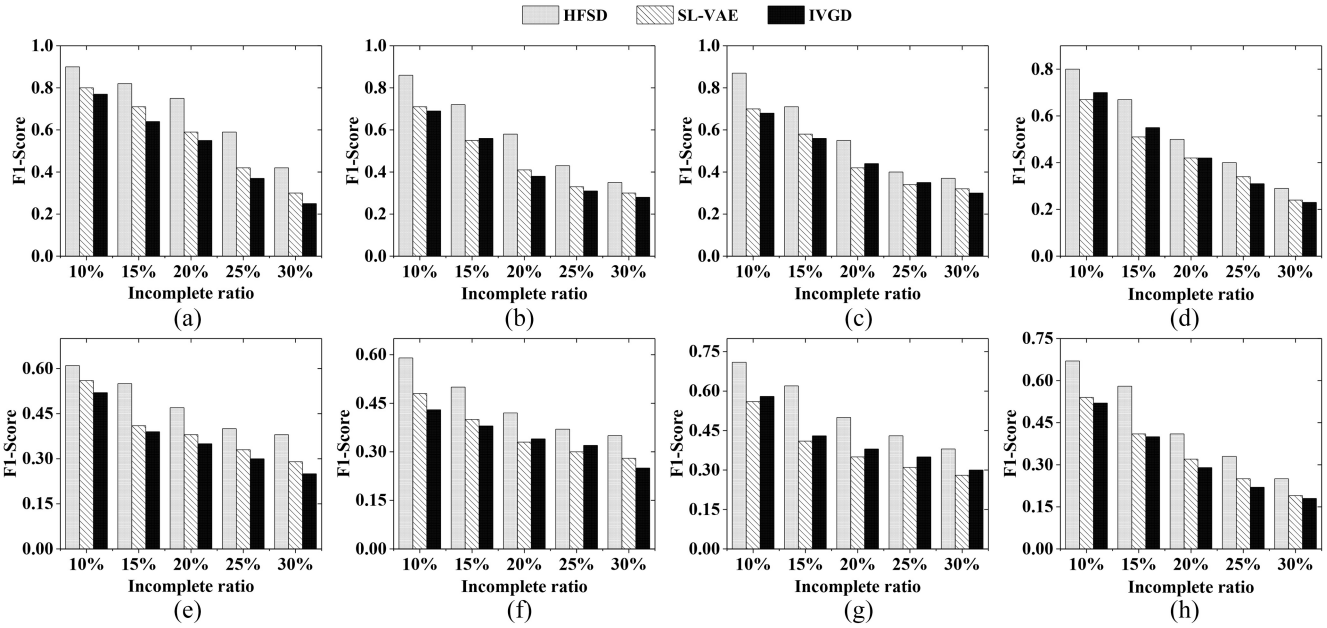

Fig. 4. Effects of data incompleteness on the SD accuracy of different methods. The selected datasets include (a) Jazz, (b) Facebook, (c) LastFM, and (d) Github, as well as (e) Android, (f) Twitter, (g) Douban, and (h) Weibo. The F1-Score is adopted as the metric.

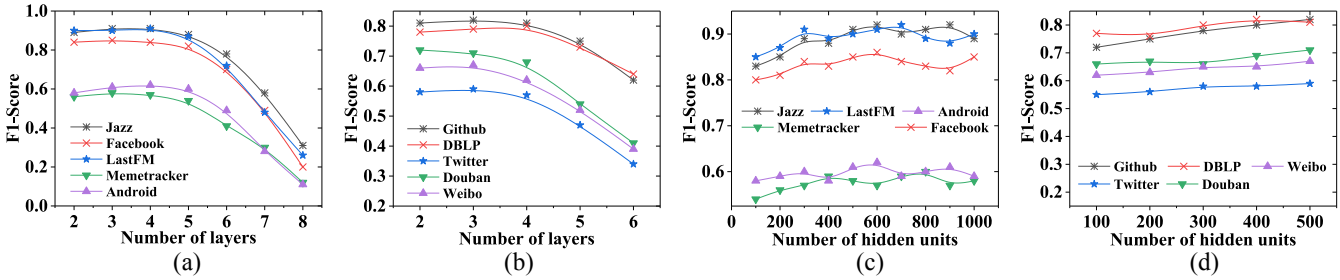

Fig. 5. Effects of the number of GAT layers and hidden units on the accuracy of the proposed HFSD under small-scale and large-scale networks. (a) and (c) Small-scale networks. (b) and (d) Large-scale networks.

and Weibo), the range is set between 2 and 6. The scale of hidden units varies from 100 to 1000 for small-scale networks and from 100 to 500 for larger-scale networks. Each parameter is isolated and tested with the other held at its optimal setting to ensure accuracy in the results. Considering computational efficiency, the number of heads in the GAT model is set to 4 for small-scale networks and reduced to 2 for larger networks. The outcomes of these experiments are quantitatively assessed using the F1-Score, with the results presented in Fig. 5.

As indicated, an inverse relationship is observed between the F1-Score and the number of layers across all datasets. Specifically, for small-scale networks, a noticeable decline in accuracy is evident when the number of layers surpasses 7. Conversely, for large-scale networks, this critical threshold is identified at five layers. This phenomenon can be attributed to the structural complexity inherent to models with n hidden layers, where each node is required to integrate representations from its n-order neighbors. Consequently, as the number of layers exceeds the aforementioned thresholds, the model's dimensionality burgeons, hindering its ability to converge within a constrained number of epochs. Furthermore, models endowed with an excessive number of layers are prone to overfitting, presenting additional challenges to achieving generalizable performance. The experimental findings also indicate that the variation in the number of hidden units exerts a negligible impact on accuracy for both small-scale and large-scale networks. This outcome is primarily due to the relatively low dimensionality of the feature space, wherein hidden layer dimensions exceeding several hundred units are deemed sufficient for capturing high-dimensional representations. Thus, while the architectural depth (i.e., the number of layers) of a model significantly influences its performance, the breadth (i.e., the number of hidden units within each layer) appears to be of lesser consequence, provided it surpasses a minimal threshold adequate for learning complex representations.

G. Model Complexity Analysis

In this study, the efficiency of HFSD, in comparison to various baseline methods, is evaluated in terms of computational time (measured in seconds). Specifically, for networks 1–6, the information diffusion dynamics are simulated using the IC model. For datasets 7–12, all propagation cascades are partitioned into training and testing sets with a ratio of 4:1. The efficiency analysis is based on the average results obtained

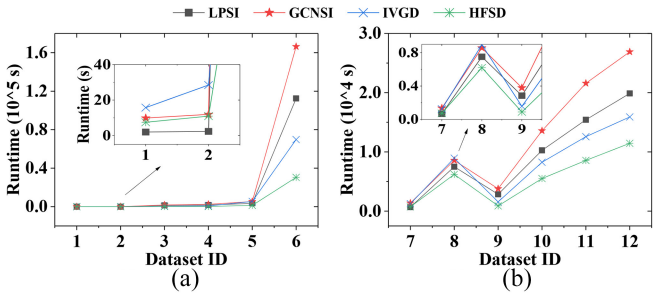

Fig. 6. Comparative analysis of running time (measured in seconds) across different methods on selected datasets. (a) Datasets 1–6. (b) Datasets 7–12.

from five independent executions. Corresponding results are presented in Fig. 6.

As demonstrated, the LPSI method, grounded in source centrality theory, exhibits superior speed on small-scale networks when compared to ML-based approaches. However, as network scale increases, ML models gradually reveal their advantages, particularly in handling larger datasets more efficiently. Among the ML-based methods, the GCNSI emerges as the most time consuming. This is primarily due to its dependency on the outputs of the LPSI method as part of its input, thus cumulatively increasing its operational time to the sum of both methods' running times. Conversely, methods that incorporate information diffusion dynamics, such as the IVGD, enhance both running time and accuracy, setting a new benchmark for SD. Nevertheless, it is observed that the running time of IVGD, which explicitly model the propagation process, significantly exceeds that of HFSD. This discrepancy highlights HFSD's superior efficiency and reduced complexity, thereby validating HFSD's ability of balancing high detection accuracy with a relatively low computational demands.

V. Conclusion

This article proposes an HFSD method aiming to address the challenges posed by the diversity and complexity of users and information in social networks. Specifically, various features of users and information are encoded into raw feature vectors to mitigate the randomness and complexity of information diffusion. Additionally, a binary classification task is performed in the final layer of the model to handle multisource detection, and a balance mechanism is designed to address differences in sample size between source and nonsource sets. Enhancing its analytical prowess, HFSD integrates a GAT, further augmenting its performance capabilities. Experimental results on diverse datasets demonstrate that HFSD outperforms baseline methods. This study extends its investigative purview to encompass the impact of different information diffusion models, propagation scale, data incompleteness, as well as the number of GAT layers and hidden units on HFSD performance. A notable observation is the inverse relationship between SD accuracy and the scale of information spread, highlighting the importance of early-stage source localization. Additionally, HFSD exhibits robust performance across different information diffusion models and data incompleteness ratios. Furthering the discourse, optimal parameter settings for the HFSD model are elucidated.

Looking ahead, this article acknowledges the model's current limitations, particularly its oversight of higher-order interactions that are emblematic of social networks. This recognition paves the way for future inquiries, advocating for the exploration of advanced modeling techniques that encapsulate the complex dynamics of social networks more comprehensively. Through this work, HFSD establishes a foundational paradigm for SD, inviting subsequent advancements and refinements within the domain.

References

[1] M. A. Manouchehri, M. S. Helfroush, and H. Danyali, "Temporal rumor blocking in online social networks: A sampling-based approach," *IEEE Trans. Syst., Man, Cybern., Syst.*, vol. 52, no. 7, pp. 4578–4588, Jul. 2022.

[2] D. Hou, C. Gao, Z. Wang, X. Li, and X. Li, "Random full-order-coverage based rapid source localization with limited observations for large-scale networks," *IEEE Trans. Netw. Sci. Eng.*, vol. 11, no. 5, pp. 4213–4226, Sep./Oct. 2024.

[3] C. Gao and J. Liu, "Network-based modeling for characterizing human collective behaviors during extreme events," *IEEE Trans. Syst., Man, Cybern., Syst.*, vol. 47, no. 1, pp. 171–183, Jan. 2017.

[4] B. Chang, E. Chen, F. Zhu, Q. Liu, T. Xu, and Z. Wang, "Maximum a posteriori estimation for information source detection," *IEEE Trans. Syst., Man, Cybern., Syst.*, vol. 50, no. 6, pp. 2242–2256, Jun. 2020.

[5] D. Zhao, L. Wang, Z. Wang, and G. Xiao, "Virus propagation and patch distribution in multiplex networks: Modeling, analysis, and optimal allocation," *IEEE Trans. Inf. Forensics Security*, vol. 14, pp. 1755–1767, 2018.

[6] C. Gao, H. Liu, J. Huang, Z. Wang, X. Li, and X. Li, "Regularized spatial–temporal graph convolutional networks for metro passenger flow prediction," *IEEE Trans. Intell. Transp. Syst.*, vol. 25, no. 9, pp. 11241–11255, Sep. 2024.

[7] Z. Jiang, X. Chen, J. Ma, and S. Y. Philip, "RumorDecay: Rumor dissemination interruption for target recipients in social networks," *IEEE Trans. Syst., Man, Cybern., Syst.*, vol. 52, no. 10, pp. 6383–6395, Oct. 2022.

[8] G. Neumann, T. Noda, and Y. Kawaoka, "Emergence and pandemic potential of swine-origin H1N1 influenza virus," *Nature*, vol. 459, no. 7249, pp. 931–939, 2009.

[9] J. Du, C. Jiang, K.-C. Chen, Y. Ren, and H. V. Poor, "Community-structured evolutionary game for privacy protection in social networks," *IEEE Trans. Inf. Forensics Security*, vol. 13, pp. 574–589, 2017.

[10] H. Kesavareddigari, S. Spencer, A. Eryilmaz, and R. Srikant, "Identification and asymptotic localization of rumor sources using the method of types," *IEEE Trans. Netw. Sci. Eng.*, vol. 7, no. 3, pp. 1145–1157, Jul–Sep. 2020.

[11] A. Guille, H. Hacid, C. Favre, and D. A. Zighed, "Information diffusion in online social networks: A survey," *ACM SIGMOD Rec.*, vol. 42, no. 2, pp. 17–28, 2013.

[12] L. Cheng, P. Zhu, K. Tang, C. Gao, and Z. Wang, "GIN-SD: Source detection in graphs with incomplete nodes via positional encoding and attentive fusion," in *Proc. AAAI Conf. Artif. Intell.*, vol. 38, 2024, pp. 55–63.

[13] P. Zhu, Q. Zhi, Y. Guo, and Z. Wang, "Analysis of epidemic spreading process in adaptive networks," *IEEE Trans. Circuits Syst. II, Exp. Briefs*, vol. 66, no. 7, pp. 1252–1256, Jul. 2019.

[14] J. Jiang, S. Wen, S. Yu, Y. Xiang, and W. Zhou, "Identifying propagation sources in networks: State-of-the-art and comparative studies," *IEEE Commun. Surveys Tuts.*, vol. 19, no. 1, pp. 465–481, 1st Quart., 2016.

[15] P. C. Pinto, P. Thiran, and M. Vetterli, "Locating the source of diffusion in large-scale networks," *Phys. Rev. Lett.*, vol. 109, no. 6, 2012, Art. no. 68702.

[16] F. Yang et al., "Locating the propagation source in complex networks with a direction-induced search based gaussian estimator," *Knowl.-Based Syst.*, vol. 195, May 2020, Art. no. 105674.

[17] W. Tang, F. Ji, and W. P. Tay, "Estimating infection sources in networks using partial timestamps," *IEEE Trans. Inf. Forensics Security*, vol. 13, pp. 3035–3049, 2018.

[18] Z. Wang, C. Wang, J. Pei, and X. Ye, "Multiple source detection without knowing the underlying propagation model," in *Proc. 31st AAAI Conf. Artif. Intell. (AAAI)*, 2017, pp. 217–223.
[19] S. S. Ali, T. Anwar, A. Rastogi, and S. A. M. Rizvi, "EPA: Exoneration and prominence based age for infection source identification," in *Proc. 28th ACM Int. Conf. Inf. Knowl. Manag.*, 2019, pp. 891–900.
[20] S. S. Ali, T. Anwar, and S. A. M. Rizvi, "A revisit to the infection source identification problem under classical graph centrality measures," *Online Soc. Netw. Media*, vol. 17, May 2020, Art. no. 100061.
[21] B. A. Prakash, J. Vreeken, and C. Faloutsos, "Spotting culprits in epidemics: How many and which ones?" in *Proc. IEEE 12th Int. Conf. Data Min.*, 2012, pp. 11–20.
[22] D. Shah and T. Zaman, "Rumors in a network: Who's the culprit?" *IEEE Trans. Inf. Theory*, vol. 57, no. 8, pp. 5163–5181, Aug. 2011.
[23] P. Hage and F. Harary, "Eccentricity and centrality in networks," *Soc. Netw.*, vol. 17, no. 1, pp. 57–63, 1995.
[24] L. C. Freeman, "Centrality in social networks conceptual clarification," *Soc. Netw.*, vol. 1, no. 3, pp. 215–239, 1978.
[25] P. Zhu, L. Cheng, C. Gao, Z. Wang, and X. Li, "Locating multi-sources in social networks with a low infection rate," *IEEE Trans. Netw. Sci. Eng.*, vol. 9, no. 3, pp. 1853–1865, May/Jun. 2022.
[26] L. Peel, T. P. Peixoto, and M. De Domenico, "Statistical inference links data and theory in network science," *Nat. Commun.*, vol. 13, no. 1, p. 6794, 2022.
[27] T. Bian et al., "Rumor detection on social media with bi-directional graph convolutional networks," in *Proc. AAAI Conf. Artif. Intell.*, vol. 34, 2020, pp. 549–556.
[28] C. Gao, J. Zhu, F. Zhang, Z. Wang, and X. Li, "A novel representation learning for dynamic graphs based on graph convolutional networks," *IEEE Trans. Cybern.*, vol. 53, no. 6, pp. 3599–3612, Jun. 2022.
[29] F. Scarselli, M. Gori, A. C. Tsoi, M. Hagenbuchner, and G. Monfardini, "The graph neural network model," *IEEE Trans. Neural Netw.*, vol. 20, no. 1, pp. 61–80, Jan. 2008.
[30] T. N. Kipf and M. Welling, "Semi-supervised classification with graph convolutional networks," in *Proc. 5th Int. Conf. Learn. Represent.*, 2017, pp. 1–14.
[31] M. Dong, B. Zheng, N. Quoc Viet Hung, H. Su, and G. Li, "Multiple rumor source detection with graph convolutional networks," in *Proc. 28th ACM Int. Conf. Inf. Knowl. Manag.*, 2019, pp. 569–578.
[32] J. Wang, J. Jiang, and L. Zhao, "An invertible graph diffusion neural network for source localization," in *Proc. ACM Web Conf.*, 2022, pp. 1058–1069.
[33] C. Ling, J. Jiang, J. Wang, and Z. Liang, "Source localization of graph diffusion via variational autoencoders for graph inverse problems," in *Proc. 28th ACM SIGKDD Conf. Knowl. Discov. Data Min.*, 2022, pp. 1010–1020.
[34] W. O. Kermack and A. G. McKendrick, "A contribution to the mathematical theory of epidemics," *Proc. Roy. Soc. London*, vol. 115, no. 772, pp. 700–721, 1927.
[35] W. O. Kermack and A. G. McKendrick, "Contributions to the mathematical theory of epidemics. II.—The problem of endemicity," *Proc. Roy. Soc. London*, vol. 138, no. 834, pp. 55–83, 1932.
[36] L. J. Allen, "Some discrete-time SI, SIR, and SIS epidemic models," *Math. Biosci.*, vol. 124, no. 1, pp. 83–105, 1994.
[37] R. M. Anderson, B. Anderson, and R. M. May, *Infectious Diseases of Humans: Dynamics and Control*. Oxford, U.K.: Oxford Univ., 1992.
[38] J. Goldenberg, B. Libai, and E. Muller, "Talk of the network: A complex systems look at the underlying process of word-of-mouth," *Market. Lett.*, vol. 12, no. 3, pp. 211–223, 2001.
[39] M. Granovetter, "Threshold models of collective behavior," *Amer. J. Sociol.*, vol. 83, no. 6, pp. 1420–1443, 1978.
[40] M. Dong, B. Zheng, G. Li, C. Li, K. Zheng, and X. Zhou, "Wavefront-based multiple Rumor sources identification by multi-task learning," *IEEE Trans. Emerg. Topics Comput. Intell.*, vol. 6, no. 5, pp. 1068–1078, Oct. 2022.
[41] R. Albert, H. Jeong, and A.-L. Barabási, "Error and attack tolerance of complex networks," *Nature*, vol. 406, no. 6794, pp. 378–382, 2000.
[42] D. K. Hammond, P. Vandergheynst, and R. Gribonval, "Wavelets on graphs via spectral graph theory," *Appl. Comput. Harmon. Anal.*, vol. 30, no. 2, pp. 129–150, 2011.
[43] M. Defferrard, X. Bresson, and P. Vandergheynst, "Convolutional neural networks on graphs with fast localized spectral filtering," in *Proc. Adv. Neural Inf. Process. Syst.*, vol. 29, 2016, pp. 1–9.
[44] P. Velickovic, G. Cucurull, A. Casanova, A. Romero, P. Lio, and Y. Bengio, "Graph attention networks," in *Proc. Int. Conf. Learn. Represent.*, 2018, pp. 1–12.
[45] Y. Rong, W. Huang, T. Xu, and J. Huang, "The truly deep graph convolutional networks for node classification," 2019, *arXiv:1907.10903*.
[46] M. Girvan and M. E. J. Newman, "Community structure in social and biological networks," *Proc. Nat. Acad. Sci.*, vol. 99, no. 12, pp. 7821–7826, 2002.
[47] P. M. Gleiser and L. Danon, "Community structure in jazz," *Adv. Complex Syst.*, vol. 6, no. 4, pp. 565–573, 2003.
[48] J. Leskovec and J. J. Mcauley, "Learning to discover social circles in ego networks," in *Proc. Adv. Neural Inf. Process. Syst.*, 2012, pp. 539–547.
[49] B. Rozemberczki and R. Sarkar, "Characteristic functions on graphs: Birds of a feather, from statistical descriptors to parametric models," in *Proc. 29th ACM Int. Conf. Inf. Knowl. Manag.*, 2020, pp. 1325–1334.
[50] B. Rozemberczki, C. Allen, and R. Sarkar, "Multi-scale attributed node embedding," *J. Complex Netw.*, vol. 9, no. 2, 2021, Art. no. cnab014.
[51] J. Yang and J. Leskovec, "Defining and evaluating network communities based on ground-truth," in *Proc. ACM SIGKDD Workshop Min. Data Semant.*, 2012, pp. 1–8.
[52] A. Sankar, X. Zhang, A. Krishnan, and J. Han, "Inf-VAE: A variational autoencoder framework to integrate homophily and influence in diffusion prediction," in *Proc. 13th Int. Conf. Web Search Data Min.*, 2020, pp. 510–518.
[53] J. Leskovec, L. Backstrom, and J. Kleinberg, "Meme-tracking and the dynamics of the news cycle," in *Proc. 15th ACM SIGKDD Int. Conf. Knowl. Discov. Data Min.*, 2009, pp. 497–506.
[54] N. O. Hodas and K. Lerman, "The simple rules of social contagion," *Sci. Rep.*, vol. 4, no. 1, p. 4343, 2014.
[55] E. Zhong, W. Fan, J. Wang, L. Xiao, and Y. Li, "ComSoc: Adaptive transfer of user behaviors over composite social network," in *Proc. 18th ACM SIGKDD Int. Conf. Knowl. Discov. Data Min.*, 2012, pp. 696–704.
[56] Q. Cao, H. Shen, K. Cen, W. Ouyang, and X. Cheng, "DeepHawkes: Bridging the gap between prediction and understanding of information cascades," in *Proc. ACM Conf. Inf. Knowl. Manag.*, 2017, pp. 1149–1158.
[57] S. N. Soffer and A. Vazquez, "Network clustering coefficient without degree-correlation biases," *Phys. Rev. E, Stat. Phys. Plasmas Fluids Relat. Interdiscip. Top.*, vol. 71, no. 5, 2005, Art. no. 57101.
[58] A. P. Bradley, "The use of the area under the ROC curve in the evaluation of machine learning algorithms," *Pattern Recognit.*, vol. 30, no. 7, pp. 1145–1159, 1997.

Le Cheng received the B.S. degree from Northwestern Polytechnical University, Xi'an, China, in 2019, where he is currently pursuing the Ph.D. degree with the School of Computer Science and also with the School of iOPEN.

His main research interests include the diffusion dynamics on complex networks, source localization, and link prediction in social networks.

Peican Zhu (Member, IEEE) received the Ph.D. degree from the University of Alberta, Edmonton, AB, Canada, in 2015.

He is currently an Associate Professor with the School of iOPEN, Northwestern Polytechnical University, Xi'an, China. His research interests include data-driven complex systems modeling, complex social networks analysis, application of AI technologies, and security of AI system.

Chao Gao received the Ph.D. degree from the Beijing University of Technology, Beijing, China, in 2010.

He is currently a Professor with the School of iOPEN, Northwestern Polytechnical University, Xi'an, China. His main research interests include data-driven complex systems modeling, complex social networks analysis, and nature-inspired computing.

Zhen Wang (Fellow, IEEE) is a Distinguished Professor and the Dean of the School of Cybersecurity, Northwestern Polytechnical University, Xi'an, China. Focusing on artificial intelligence, networks, multiagent systems, and games, he has published more than 100 papers in PNAS, *Science Advances*, *Nature Communications*, *Physical Review Letters*, IEEE TRANSACTIONS ON PATTERN ANALYSIS AND MACHINE INTELLIGENCE, IEEE/ACM TRANSACTIONS ON NETWORKING, IEEE TRANSACTIONS ON INFORMATION FORENSICS AND SECURITY, IEEE TRANSACTIONS ON NEURAL NETWORKS AND LEARNING SYSTEMS, IEEE TRANSACTIONS ON CYBERNETICS, IEEE TRANSACTIONS ON KNOWLEDGE AND DATA ENGINEERING, NeurIPs, ICLR, ICML, WWW, IJCAI, and AAAI with over 30 000 citations.

Dr. Wang is an Elected Member of Academia Europaea/The Academy of Europe and European Academy of Sciences and Arts, and a Fellow of AAIA and IOP.

Xuelong Li (Fellow, IEEE) is a Full Professor with the School of Artificial Intelligence, Optics and Electronics (iOPEN), Northwestern Polytechnical University, Xi'an, China.